

Scanning and non-scanning surface plasmon microscopy to observe cell adhesion sites

Koyo Watanabe,^{1,*} Koji Matsuura,¹ Fukukazu Kawata,² Kotaro Nagata,² Jun Ning,³ and Hiroshi Kano^{2,3}

¹Research Core for Interdisciplinary Sciences, Okayama University, 3-1-1 Tsushima-Naka, Kita-Ku Okayama 700-8530, Japan

²Division of Information and Electronic Engineering, Graduate School of Engineering, Muroran Institute of Technology, Mizumoto 27-1, Muroran, Hokkaido 050-8585, Japan

³Division of Engineering for Composite Functions, Graduate School of Engineering, Muroran Institute of Technology, Mizumoto 27-1, Muroran, Hokkaido 050-8585, Japan

*koyouwatanabe@gmail.com

Abstract: We observe adhesion sites of a cell on a substrate with high resolution. Since this observation requires interfacial measurements between the cell and the substrate, we employ scanning localized surface plasmon microscopy. We experimentally show that focal adhesion sites of a mouse muscle cell can be observed without fluorescent labeling. We also show that a non-scanning surface plasmon microscope combined with the scanning localized surface plasmon microscope contributes to observing an entire cell adhesion site and identify regions of interest.

© 2012 Optical Society of America

OCIS codes: (240.6680) Surface plasmons; (180.4243) Near-field microscopy; (170.1530) Cell analysis.

References and links

1. A. J. Ridley, M. A. Schwartz, K. Burridge, R. A. Firtel, M. H. Ginsberg, G. Borisy, J. T. Parsons, and A. R. Horwitz, "Cell migration: integrating signals from front to back," *Science* **302**(5651), 1704–1709 (2003).
2. N. L. Perillo, M. E. Marcus, and L. G. Baum, "Galectins: versatile modulators of cell adhesion, cell proliferation, and cell death," *J. Mol. Med.* **76**(6), 402–412 (1998).
3. J. Folkman and A. Moscona, "Role of cell shape in growth control," *Nature* **273**(5661), 345–349 (1978).
4. M. E. Chicurel, C. S. Chen, and D. E. Ingber, "Cellular control lies in the balance of forces," *Curr. Opin. Cell Biol.* **10**(2), 232–239 (1998).
5. C. Zhong, M. Chrzanoska-Wodnicka, J. Brown, A. Shaub, A. M. Belkin, and K. Burridge, "Rho-mediated contractility exposes a cryptic site in fibronectin and induces fibronectin matrix assembly," *J. Cell Biol.* **141**(2), 539–551 (1998).
6. O. Medalia and B. Geiger, "Frontiers of microscopy-based research into cell-matrix adhesions," *Curr. Opin. Cell Biol.* **22**(5), 659–668 (2010).
7. B. Rothenhäusler and W. Knoll, "Surface-plasmon microscopy," *Nature* **332**(6165), 615–617 (1988).
8. A. W. Peterson, M. Halter, A. Tona, K. Bhadriraju, and A. L. Plant, "Surface plasmon resonance imaging of cells and surface-associated fibronectin," *BMC Cell Biol.* **10**(1), 16 (2009).
9. J. Homola, *Surface Plasmon Resonance Based Sensors* (Springer, 2006).
10. W. Hickel and W. Knoll, "Surface plasmon microscopy of lipid layers," *Thin Solid Films* **187**(2), 349–356 (1990).
11. C. E. H. Berger, R. P. H. Kooyman, and J. Greve, "Resolution in surface plasmon microscopy," *Rev. Sci. Instrum.* **65**(9), 2829–2836 (1994).
12. H. Raether, *Surface Plasmons on Smooth and Rough Surfaces and on Gratings* (Springer, 1988).
13. N. Q. Balaban, U. S. Schwarz, D. Riveline, P. Goichberg, G. Tzur, I. Sabanay, D. Mahalu, S. Safran, A. Bershadsky, L. Addadi, and B. Geiger, "Force and focal adhesion assembly: a close relationship studied using elastic micropatterned substrates," *Nat. Cell Biol.* **3**(5), 466–472 (2001).
14. U. S. Schwarz, N. Q. Balaban, D. Riveline, L. Addadi, A. Bershadsky, S. A. Safran, and B. Geiger, "Measurement of cellular force at focal adhesions using elastic micro-patterned substrates," *Mater. Sci. Eng. C* **23**(3), 387–394 (2003).
15. H. Kano and W. Knoll, "A scanning microscope employing localized surface-plasmon-polaritons as a sensing probe," *Opt. Commun.* **182**(1-3), 11–15 (2000).
16. K. Watanabe, N. Horiguchi, and H. Kano, "Optimized measurement probe of the localized surface plasmon microscope by using radially polarized illumination," *Appl. Opt.* **46**(22), 4985–4990 (2007).

17. K. Watanabe, M. Ryosuke, G. Terakado, T. Okazaki, K. Morigaki, and H. Kano, "High resolution imaging of patterned model biological membranes by localized surface plasmon microscopy," *Appl. Opt.* **49**(5), 887–891 (2010).
18. F. Kawata, R. Miyazaki, G. Terakado, K. Watanabe, and H. Kano, "Scanning and non-scanning surface plasmon microscopy of refractive index distribution on a metal surface," in *Focus on Microscopy* (Focus on Microscopy Society, 2011), abstract 269.
19. A. Yamada, Y. Katanosaka, S. Mohri, and K. Naruse, "A rapid microfluidic switching system for analysis at the single cellular level," *IEEE Trans. Nanobioscience* **8**(4), 306–311 (2009).
20. B. A. McCool, J.-P. Pin, P. F. Brust, M. M. Harpold, and D. M. Lovinger, "Functional coupling of rat group II metabotropic glutamate receptors to an ω -conotoxin GVIA-sensitive calcium channel in human embryonic kidney 293 cells," *Mol. Pharmacol.* **50**(4), 912–922 (1996).
21. K. M. Yamada, R. Pankov, and E. Cukierman, "Dimensions and dynamics in integrin function," *Braz. J. Med. Biol. Res.* **36**(8), 959–966 (2003).
22. L. Formigli, E. Meacci, C. Sassoli, F. Chellini, R. Giannini, F. Quercioli, B. Tiribilli, R. Squecco, P. Bruni, F. Francini, and S. Zecchi-Orlandini, "Sphingosine 1-phosphate induces cytoskeletal reorganization in C2C12 myoblasts: physiological relevance for stress fibres in the modulation of ion current through stretch-activated channels," *J. Cell Sci.* **118**(6), 1161–1171 (2005).
23. H. Y. Li, E. K. O. Ng, S. M. Y. Lee, M. Kotaka, S. K. W. Tsui, C. Y. Lee, K. P. Fung, and M. M. Y. Waye, "Protein-protein interaction of FHL3 with FHL2 and visualization of their interaction by green fluorescent proteins (GFP) two-fusion fluorescence resonance energy transfer (FRET)," *J. Cell. Biochem.* **80**(3), 293–303 (2001).

1. Introduction

Cell adhesion sites, which mediate the interface between cells and the surrounding tissues, play an essential role in activating cellular functions, such as signal communication, embryonic morphogenesis, and cell proliferation [1,2]. With the exception of cancer cells, non-adherent cells undergo apoptosis [3]. It is assumed that the movement of focal adhesion sites (e.g., the motion of integrin receptors) triggers cellular activation, which is induced by the unfolding of domains in the integrin itself [4] or in associated membrane molecules [5]. Thus, the microscopic observation of these sites is essential for understanding the fundamental processes of cellular activation. Clarifying the mechanism of adhesion is a great challenge to those attempting to advance life sciences.

Among the various types of microscopes used in cell adhesion research [6], the non-scanning surface plasmon microscope, which is a lens-imaging-type surface plasmon microscope (LISPM) [7,8], is recognized as a powerful tool because LISPM yields high-contrast images against refractive index variations and the measurement depth is confined within a few hundred nanometers from the substrate surface [9]. These features allow the selective observation of adhesion sites, even when they are sandwiched between the cell and the substrate. Furthermore, LISPM is applicable to measurements of an unlabeled sample in an aqueous environment without physical contact [9]. These features render the surface plasmon microscope highly attractive to those performing cell adhesion research as well as those observing the underlying supports.

The disadvantage of using LISPM for observing focal adhesions is its spatial resolution [10–12]. Since the typical size of the focal adhesion sites is $\sim 1\ \mu\text{m}$ [13,14], a spatial resolution of $\sim 10\ \mu\text{m}$ is inadequate. This problem can be resolved by employing the scanning localized surface plasmon microscope (SLSPM) [15], which achieves a high spatial resolution of $\sim 200\ \text{nm}$ by using a locally excited surface plasmon as a sensing probe [16,17]. The SLSPM can thus contribute in further improvement of our understanding on the focal adhesion sites.

Although LISPM has a limited spatial resolution, it still remains useful for observing whole cells and groups of cellular adhesion sites because LISPM easily expands an observing area. We expect that the advantage of SLSPM will be heightened when it is combined with LISPM.

We herein introduce an optical system that can switch between LISPM and SLSPM to exploit the advantages of both microscopes. We describe the imaging principles and properties of both microscopes and show observed images of focal adhesion sites in mouse muscle cells.

2. LISPM and SLSPM

Figure 1 shows an optical system that combines LISPM and SLSPM [18]. The two microscopes can be switched by using flipper mirrors FM1 and FM2. Figure 1(a) shows the optical path in the LISPM, where a polarized He-Ne laser operated at a wavelength of 632.8 nm is used as a light source. The laser light is expanded and collimated with a set of lenses labeled L1 and L2. The expanded light is reflected by the flipper mirror FM1 and the mirror M1 and focused by L3 onto the entrance pupil of an oil-immersion objective lens (N.A. = 1.65). The light passing through the objective lens illuminates the substrate as a plane wave. The polarization and incident angle of the plane wave can be controlled by the position of the focused light on the pupil. The light reflected from the metal surface is projected onto CCD1 via the objective lens and L4 to give an image of the metal film surface.

In the case of the LISPM, the reflectance at a certain microscopic region decreases when the incident angle of p-polarized illumination coincides with the excitation angle of the surface plasmon. Thus, image contrast results from the variation of the refractive index on the surface.

Figure 1(b) shows the optical path in the SLSPM, which employs the same light source and set of lenses labeled L1 and L2. The polarization of the expanded light is converted from linear to quasi-radial using a Z-Pol (Nanophoton, Japan). The output light is relayed onto the entrance pupil of the oil immersion objective lens by a Telecentric imaging system (L5 and L6). The relayed light is focused on the substrate surface. The reflected light is collected by the same objective lens. The exit pupil of the objective lens is imaged onto the CCD2 by L7. The intensity distribution recorded by the CCD2 is then transferred to a PC. The substrate is scanned in two dimensions using a piezo-stage.

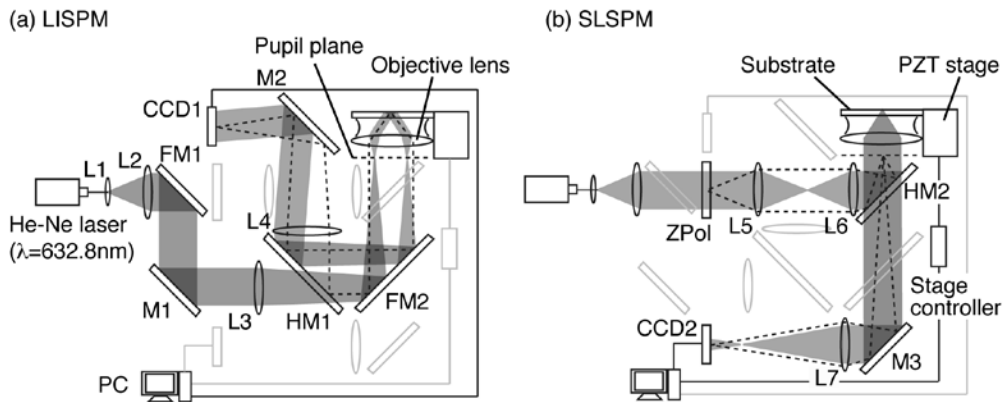


Fig. 1. The optical systems of (a) the lens imaging surface plasmon microscope (LISPM) and (b) the scanning localized surface plasmon microscope (SLSPM). The optical paths can be switched using the flipper mirrors FM1 and FM2.

In the case of the SLSPM, a series of the pupil images are processed to create an image visualizing variations of the refractive index. As shown in Fig. 2(a), an absorption ring with a certain radius appears in the typical pupil image because of the excitation of surface plasmons. Since its radius depends on the refractive index at the surface, the light intensities near the circular absorption pattern reflects variation of the refractive index [12]. The details of the processing procedures are as follows: (a) select a pupil image as a reference; (b) find the best fit ring to the absorption pattern in the selected pupil image; (c) fix the center and the radius of the ring; (d) find pixels containing a portion of the best fit ring inside in each of the pupil images. (Fig. 2 (b) is a magnified section of the pupil image); (e) sum up the pixel values by giving weights that are proportional to the length of the ring segment in each pixel; and (f) normalize the sum by the circumference of the ring. The normalized value was assigned to a corresponding pixel of the SLSPM image.

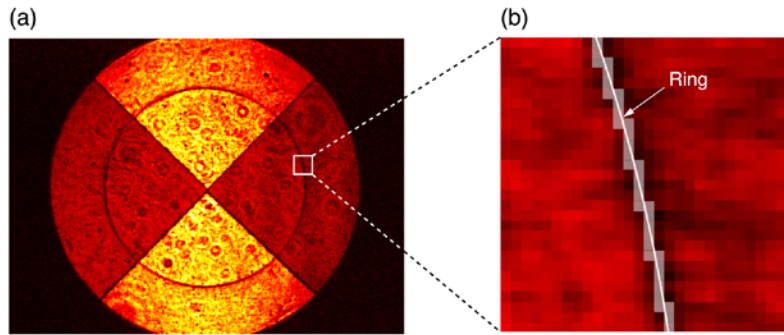


Fig. 2. (a) Reflected light intensity distribution in the pupil plane. (b) Magnified image of squared area shown in (a). The pixels that overlapped with a ring (white line) were highlighted using semitransparent white shading.

We demonstrated the imaging properties of LISPM and SLSPM by observing latex particles. We prepared a substrate that consisted of a cover glass and a 44-nm-thick gold film. We distributed the particles of size $1.053\ \mu\text{m}$ onto the gold film. For this observation, we set the illumination angle to an excitation angle of surface plasmons in a particle-free region of the metal surface, and made the plane wave p-polarized. Figure 3 shows the particle image produced by the LISPM. The image shows several particles with a comet-like tails extending along the direction of arrow A in Fig. 3. This direction coincides with that of the incoming plane wave. We can also see an interference pattern in region where two of the tails overlap. This interference suggests that a detailed structure cannot be determined by LISPM when the sample is aggregated. Despite this disadvantage, LISPM is useful for identifying sites suitable for the SLSPM imaging because LISPM allows an instantaneous observation over an entire cell.

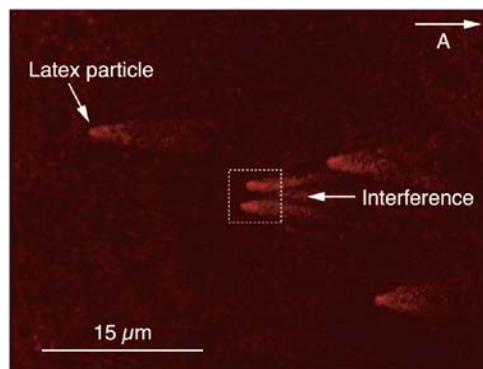


Fig. 3. LISPM image of latex particles with a diameter of $1.053\ \mu\text{m}$. The arrow A shows the propagation direction of surface plasmons.

Figure 4 shows an SLSPM image of the particles located in the frame in Fig. 3. The scanning range is $5\ \mu\text{m} \times 5\ \mu\text{m}$, and the scanning points are 64×64 . The image shows highly resolved particles with a high contrast. The SLSPM image is also free of the comet-like tails. Thus, the combination of two microscopes provides us with more opportunities to identify sites of interest and acquire their detailed structure.

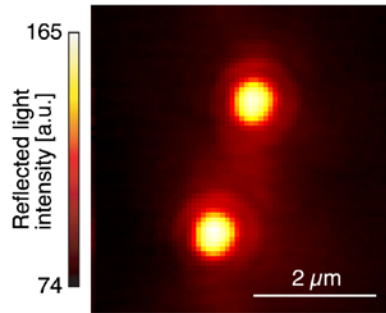


Fig. 4. SLSPM image of latex particles with a diameter of 1.053 μm . The observed area corresponds to the framed area shown in Fig. 3.

3. Preparation of substrate and cells

We prepared a substrate that consisted of a cover glass, a gold layer, and a SiO_2 layer. The gold layer was deposited onto the cleaned glass substrate by an evaporator (AUTO306, Edwards) to a thickness of 44 nm. The SiO_2 was sputtered onto it to a thickness of 12 nm (RFS-200, ULVAC, Japan). A mouse myoblast cell line (C2C12) was chosen as the cell sample because it adheres to the SiO_2 surface with no extracellular matrix. The C2C12 cell helps to simplify measurement of the substrate surface. C2C12 cells were cultured using Dulbecco's modified eagle's medium (DMEM; Sigma) and maintained in an incubator with 5% CO_2 at 37°C [19,20]. After incubation, the culture medium surrounding the C2C12 cells was removed, and the cells were washed twice with 10 ml of phosphate buffer solution (Wako, Japan). To remove the C2C12 cells from the laboratory dish, 1 ml of 1% trypsin solution was added to the C2C12 cell and immediately recovered. Subsequently, 10 ml DMEM was added to the culture dish and the detached cells were collected. The suspension of the cells was placed on the SiO_2 surface of the substrate, after cleaning the substrate surface with ultraviolet irradiation. The prepared C2C12 cells were again cultured with 5% of CO_2 at 37°C overnight. They were then soaked in 4% paraformaldehyde solution (Nakarai Tesque, Japan), and gradually dried.

4. Results and discussion

Figure 5 shows a C2C12 cell image observed with the LISPM, showing an entire fixed cell on the substrate. There is a point, where the cell diverges in two directions. Although the

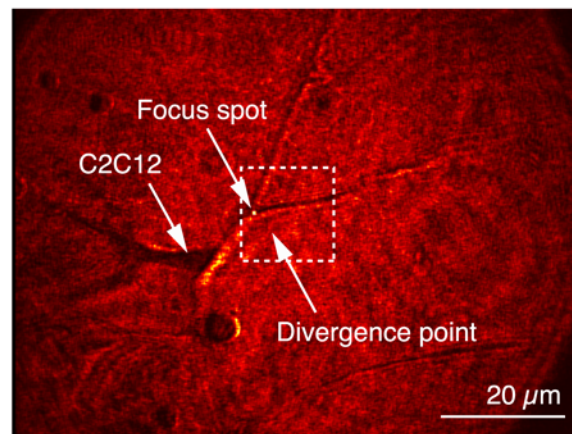


Fig. 5. Observed LISPM image of the underlying supports of a mouse muscle cell. The white arrows indicate the C2C12 cell and the cellular divergence point. The framed area is the section observed by SLSPM as shown in Fig. 6.

divergence point is observed, the focal adhesion sites with submicron size are not visible. To observe the detailed structure, we switched over to the SLSPM. Since the flipper mirror FM1 in Fig. 1(a) transmits a small amount of light, the imaging area can be located by finding a focus spot of the light traveling along the path of the SLSPM.

We expected to find focal adhesion sites around the divergence point because cells need anchors to grow and divide [21]. We therefore imaged the boxed area in Fig. 5 by SLSPM. Figure 6 shows the result. The observed area was $15\ \mu\text{m} \times 15\ \mu\text{m}$. The scanning points were 64×64 . The outline of the cellular divergence is consistent with the outline in the LISPM image. The white circles in Fig. 6 indicate several round structures $\sim 1\ \mu\text{m}$ in diameter, which could not be resolved in the LISPM image. They are visible only inside the cell and not outside. These characteristics are consistent with properties of focal adhesion sites observed with a fluorescence microscope [22,23] or a transmission electron microscope [6]. Another submicron-size structure is observed along the dashed line A. This shows a linear structure with a width of $\sim 400\ \text{nm}$. These results demonstrate the usefulness of SLSPM for observing the submicron structures of underlying cellular supports and focal adhesion sites without fluorescent dyes or proteins.

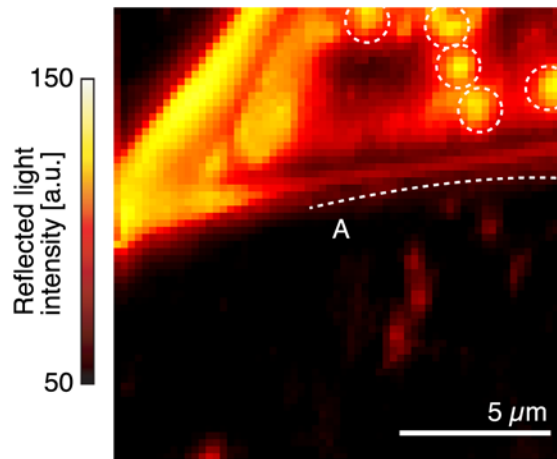


Fig. 6. SLSPM image observed at divergence point of the C2C12 cell.

5. Conclusion

We have proposed an optical system that combines scanning localized surface plasmon microscopy and non-scanning surface plasmon microscopy. We have shown that the system allows wide field and highly resolved imaging by switching between the non-scanning and scanning microscopes by observing latex particles with a diameter of $1.053\ \mu\text{m}$. We have also shown that the LISPM can be used to find the divergence area of a C2C12 cell and that the SLSPM can then be used to observe the focal adhesion sites on the SiO_2 .

Acknowledgments

This study was partly supported by a Grant-in-Aid for Scientific Research for Young Scientists (A) (No. 22680036 to K.M.) and by the Special Coordination Funds for Promoting Sciences and Technology from the Ministry of Education, Science, Sports, and Culture, Japan. We would like to thank Ms. Ikuyo Sugimoto for her assistance in the culture and preparation of C2C12 cells. We also would like to thank Takefumi Kanda and Yuichi Ashida (Okayama University, Japan) for helping with SiO_2 sputtering.